Resonant Layer Responses to Non-Axisymmetric Magnetic Perturbations in Two-Fluid, Drift-MHD Regimes

Yeongsun Lee[1], Jong-Kyu Park[1,2], Jace Waybright[2], and Yong-Su Na[1]

[1] *Department of Nuclear Engineering, Seoul National University, Seoul, South Korea.*
[2] *Princeton Plasma Physics Laboratory, Princeton, New Jersey, USA*

1. Introduction

A tokamak responds strongly to non-axisymmetric, resonant magnetic perturbations (hereafter will be referred to as RMP for brevity) through a narrow layer across a rational surface as seen in magnetic reconnection and braking. RMP is a promising scheme to ensure stable and high-performance operations in tokamaks [1, 2, 3, 4] such as to correct intrinsic error fields, mitigate and suppress ELMs in H-mode plasmas and runaway electrons during tokamak disruptions. Therefore, in-depth understanding of resonant layer responses is of great importance in exploring the fidelity of the fusion reactors.

The perturbed responses can be characterized by the single parameter Δ, which quantifies the discontinuity in the magnetic field normal to the resonant surface and represents the shielding currents across the resonant layer. Inherent complexity in the responses necessitates adopting the two-fluid drift-MHD model in the complete form. For instance, including electron viscosity in the generalized Ohm's law alters the power-law exponent of electron density in the penetration threshold from 1/4 [5] to 5/8 [6] or 1/4 [5] to 11/16 [7], depending on the regime transitions (SCi → SCiPe, HRi → EV, respectively). Similarly, it was recently unveiled that the parallel flow response gives rise to the ion shielding current and shifts the zero-crossing condition of Δ for $\mathrm{E}\times\mathrm{B}$ rotation. In this work, we explore the complex responses by employing the code, Slab-Layer (SLAYER) [8] which incorporates various physics in the two-fluid drift-MHD regimes. The intrinsic numerical stiffness is successfully addressed using the higher-order Riccati transformation method adapted to the layer problem [9].

2. Layer Physics

The four-field model, deduced from the reduction and normalization of the two-fluid drift-MHD equations, read

$$i(Q-Q_e)\tilde{\psi} = iX\left(\tilde{\phi}-\tilde{Z}\right) + \frac{d^2\tilde{\psi}}{dX^2} - (1+\tau)P_e\left(\frac{d^2\tilde{V}_z}{dX^2} + \frac{D^2}{c_\beta^2}\frac{d^4\tilde{\psi}}{dX^4}\right)\cdots(1),$$

$$iQ\tilde{Z} = iQ_e\tilde{\phi} + iD^2X\frac{d^2\tilde{\psi}}{dX^2} + ic_\beta^2X\tilde{V}_z + \left(c_\beta^2+\left(1-c_\beta^2\right)K\right)\frac{d^2\tilde{Z}}{dX^2} + P_eD^2\left(\frac{d^4\tilde{\phi}}{dX^4} - \frac{d^4\tilde{Z}}{dX^4}\right)\cdots(2),$$

$$i(Q-Q_i)\frac{d^2\tilde{\phi}}{dX^2}=iX\frac{d^2\tilde{\psi}}{dX^2}+P\left(\frac{d^4\tilde{\phi}}{dX^4}+\tau\frac{d^4\tilde{Z}}{dX^4}\right)+P_e\left(\frac{d^4\tilde{\phi}}{dX^4}-\frac{d^4\tilde{Z}}{dX^4}\right)\cdots(3),$$

$$iQ\tilde{V}_z=-iQ_e\tilde{\psi}+iX\tilde{Z}+P\frac{d^2\tilde{V}_z}{dX^2}+P_e\left(\frac{d^2\tilde{V}_z}{dX^2}+\frac{D^2}{c_\beta^2}\frac{d^4\tilde{\psi}}{dX^4}\right)\cdots(4).$$

Constraining $\tilde{\psi}$ to have a tearing parity (even) results in odd parities in $\tilde{\phi}$ and $\tilde{Z}$ and an even parity in $\tilde{V}_z$. The four fields have the asymptotic behavior such that $\tilde{\psi}\to\Psi\left[1+\frac{\hat{\Delta}}{2}|X|+O\left(\frac{1}{X}\right)\right], \tilde{\phi}\to\frac{\mathrm{Q}}{\mathrm{X}}\tilde{\psi}, \tilde{Z}\to\frac{\mathrm{Q_e}}{\mathrm{X}}\tilde{\psi}$ and $\tilde{V}_z\to O\left(\frac{1}{X^3}\right)$. The amount of the reconnected flux in the slab geometry is

$$\Psi(t)=\frac{\Delta_{sw}\Xi(t)}{\Delta-\Delta_{ss}},$$

where $\Delta_{ss}=-\frac{2k}{\tanh k}$, $\Delta_{sw}=\frac{2k}{\sinh k}$ and Ξ is the amplitude of external perturbation at the edge. According to the quasi-linear force balance, the exact solution of $E\times B$ rotation at the layer is

$$V(x)=V_0-\frac{k}{2\mu_i}|\Psi|^2\Im(\Delta)(1-|x|).$$

Equations 1-4 can be solved by the two-layer matching method [5, 6] in phase space. For the verification purpose, some of analytic asymptotes are listed in Table 1.

	$\hat{\Delta}$		$\hat{\Delta}$
VRi	$\frac{6^{\frac{2}{3}}\pi\,\Gamma\left(\frac{5}{6}\right)}{\Gamma\left(\frac{1}{6}\right)}[i(Q-Q_i)]^{\frac{1}{6}}[i(Q-Q_e)]^{\frac{5}{6}}P^{\frac{1}{6}}$	VRii	$\frac{6^{\frac{2}{3}}\pi\,\Gamma\left(\frac{5}{6}\right)}{\Gamma\left(\frac{1}{6}\right)}[i(Q-Q_e)]P^{\frac{1}{6}}$
SCi	$\pi\,\frac{[i(Q-Q_i)]^{\frac{1}{2}}[i(Q-Q_e)}{D\sqrt{1+\tau}}$	HRi	$\frac{2\pi\,\Gamma\left(\frac{3}{4}\right)}{\Gamma\left(\frac{1}{4}\right)}\frac{c_\beta^{\frac{1}{2}}[i(Q-Q_e)]}{(\tau+1)^{\frac{1}{4}}D^{\frac{1}{2}}}$
SCiPe	$\frac{1.48i^{\frac{7}{4}}\pi c_\beta^{\frac{1}{2}}(Q-Q_e)(Q-Q_i)^{\frac{3}{4}}}{D^2(\tau+1)P_e^{\frac{1}{4}}}$	EV	$\frac{3\pi\,\Gamma\left(\frac{5}{8}\right)}{8^{\frac{3}{4}}\Gamma\left(\frac{11}{8}\right)}\frac{c_\beta^{\frac{5}{4}}[i(Q-Q_e)]}{(\tau+1)^{\frac{5}{8}}D^{\frac{5}{4}}P_e^{\frac{1}{4}}}$

Table 1. List of $\hat{\Delta}$. The VRi, VRii, SCi and HRi regimes were found in Ref. [5], SCiPe in Ref. [6] and EV in Ref. [7], respectively.

3. Variable transformation

We found the variable transformation adequate for minimizing the number of singularity due to inverse-viscosity ($\frac{1}{P}$ and $\frac{1}{P_e}$). According to this, the Y vector for ordinary differential system is

$$Y=[y_1^T,y_2^T]^T, y_1=\left[\tilde{\psi},\ddot{\tilde{\psi}},\dot{\tilde{\phi}},\dot{\tilde{Z}},\tilde{\xi}',\tilde{\eta}',\tilde{V}_z\right]^T \text{ and } y_2=\left[\dot{\tilde{\psi}},P_e\frac{D^2}{c_\beta^2}\dddot{\tilde{\psi}},\tilde{\phi},\tilde{Z},\tilde{\xi},\tilde{\eta},P\dot{\tilde{V}}_z\right]^T \cdots (5)$$

where $\tilde{\xi}=\ddot{\tilde{\phi}}-\ddot{\tilde{Z}}, \tilde{\xi}'=P_e\left(\dddot{\tilde{\phi}}-\dddot{\tilde{Z}}\right), \tilde{\eta}=\ddot{\tilde{\phi}}+\tau\ddot{\tilde{Z}}$ and $\tilde{\eta}'=P\left(\dddot{\tilde{\phi}}+\tau\dddot{\tilde{Z}}\right)$. The four field equations (Equations 1-4) are written with the transformed variable as

$$\frac{d}{dX}\left(P\frac{d}{dX}\tilde{V}_z\right)=i\frac{Q-Q_i}{1+\tau}\tilde{\psi}-\frac{1}{1+\tau}\frac{d^2\tilde{\psi}}{dX^2}-i\frac{X}{1+\tau}\tilde{\phi}-i\frac{\tau X}{1+\tau}\tilde{Z}+iQ\tilde{V}_z, \cdots (6)$$

$$\frac{d}{dX}\left(P_e\frac{D^2}{c_\beta^2}\frac{d^3\tilde{\psi}}{dX^3}\right)=-i\frac{Q-Q_e+\alpha(Q-Q_i)}{1+\tau}\tilde{\psi}+\frac{1+\alpha}{1+\tau}\frac{d^2\psi}{dX^2}$$

$$+i\frac{(1+\alpha)X}{1+\tau}\tilde{\phi}+i\frac{(\tau\alpha-1)X}{1+\tau}\tilde{Z}-i\alpha Q\tilde{V}_z, \cdots (7)$$

$$\frac{d}{dX}\tilde{\xi}'=-iX\frac{d^2\tilde{\psi}}{dX^2}-i\frac{Q_e}{D^2}\tilde{\phi}+i\frac{Q}{D^2}\tilde{Z}-i\frac{c_\beta^2}{D^2}X\tilde{V}_z+\frac{c_\beta^2+\left(1-c_\beta^2\right)K}{(1+\tau)D^2}\left(\tilde{\xi}-\tilde{\eta}\right), \cdots (8)$$

$$\frac{d}{dX}\tilde{\eta}'=i\frac{Q_e}{D^2}\tilde{\phi}-i\frac{Q}{D^2}\tilde{Z}+i\frac{c_\beta^2}{D^2}X\tilde{V}_z+\frac{i\tau(Q-Q_i)D^2-\left(c_\beta^2+\left(1-c_\beta^2\right)K\right)}{(1+\tau)D^2}\tilde{\xi}$$

$$+\frac{i(Q-Q_i)D^2+\left(c_\beta^2+\left(1-c_\beta^2\right)K\right)}{(1+\tau)D^2}\tilde{\eta}\cdots (9).$$

The matrix A for the ODE system is obtained according to selection of the Y vector given by equation (5) such that $Y'=AY$.

4. Resonant layer response

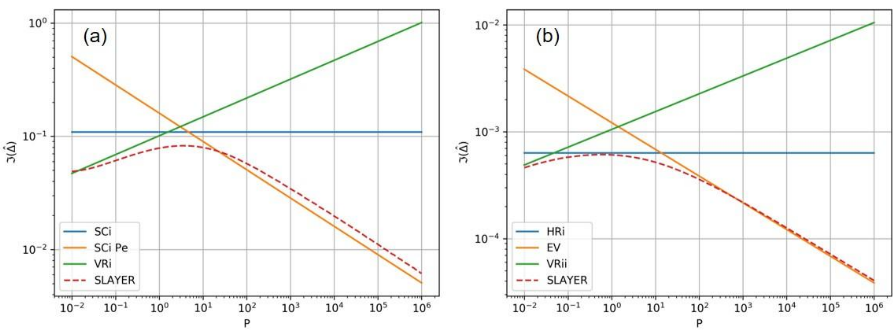

Figure 1. $Q=0.08$ **and** $Q=10^{-3}$ **in (a) and (b), respectively. For both,** $Q_e=\frac{Q}{2}, Q_i=-\frac{Q}{2}, D=0.2, c_\beta=0.1$ **and** $\frac{P_e}{P}=0.0165$**.**

Equations (6-9) are solved by SLAYER which applies the higher-order Riccati transformation method adapted to the layer problem [9]. The primary improvement from Ref. [9] is to include the electron viscosity. The implementation is verified in Figure 1 by showing agreement with the analytic asymptotes listed in Table 1 during transitions toward the high viscosity regimes (SCiPe and EV). The ion screening term is neglected in this verification since it's not accounted in the listed solutions.

The zero-crossing condition of Δ for $E \times B$ rotation, which we denote Q_{nat}, had been predicted as Q_e without the ion screening [5]. Yet, in Ref. [9], it was reported that, Q_{nat} is shifted toward the ion diamagnetic flow direction, representing the shifted natural frequency. Indeed, Figure 2. demonstrates this shift $(Q_e - Q_{nat})$ is universal in wide parametric (c_β, D) domain if the plasma flow is slow enough. This shift changes the profile of magnetic braking force as a function of Q, and contribute to enhancing the field penetration threshold particularly when $Q > Q_0$ and quasi-linear formulation of force-balance is valid [9].

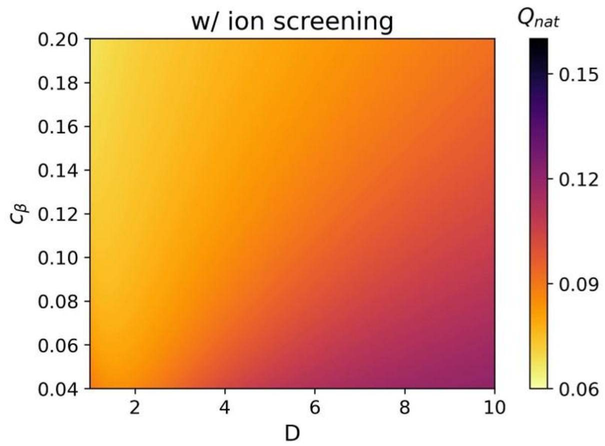

Figure 2. The contour of Q_{nat}. $Q_e = 0.15, Q_i = -0.15$ and $P = 1$ are used. All values of Q_{nat} are evidently shifted from the prediction without the ion screening, i.e. Q_e.

This work is supported by the Technology Development Projects for Leading Nuclear Fusion through the National Research Foundation of Korea (NRF) funded by the Ministry of Science and ICT (No. RS-2024-00281276). This research was supported by R&D Program of "Optimal Basic Design of DEMO Fusion Reactor, CN2502-1" through the Korea Institute of Fusion Energy (KFE) funded by the Government funds.

[1] Jong-Kyu Park et al., 2018 *Nat. Physics* **14** 1233-1228

[2] M. Lehnen et al., 2008 *Phys. Rev. Lett.* **100** 25503

[3] SangKyeun Kim et al., 2024 *Nat. Commun.* **15** 3990

[4] SeongMoo Yang et al., 2024 *Nat. Commun.* **15** 1275

[5] A. Cole and R. Fitzpatrick 2006 *Phys. Plasmas* **13** 032503

[6] J. C. Waybright and J.-K. Park 2024 *Phys. Plasmas* **31** 222502

[7] Yeongsun Lee, Jace Waybright and Jong-Kyu Park, *Phys. Plasmas* (submitted)

[8] Jong-Kyu Park 2022 *Phys. Plasmas* **29** 072506

[9] Yeongsun Lee *et al* 2024 *Nucl. Fusion* **10** 106058